

Quantification of Partial Volume Effects in Salivary Glands SPECT Images after Radiation Therapy of Head and Neck Tumors

MpumeleloNyathi^{1*}

1. Department of Medical Physics, Faculty of Health Sciences, Sefako Makgatho Health Sciences University, Gauteng, South Africa

ARTICLE INFO	ABSTRACT
<p>Article type: Original Article</p>	<p>Introduction: Radical radiation therapy of head and neck cancers may injure the salivary glands and reduce their function. Single-photon emission computed tomography (SPECT) images maybe used to evaluate function post-therapy. However, accurate quantification is hindered by the partial volume effects (PVEs). The present study involved the introduction of a PVEs quantification technique aimed at improved quantification of the salivary glands function.</p> <p>Material and Methods: The parotid and submandibular salivary glands were mimicked with hollow spheres. The left parotid (LP), right parotid (RP), left submandibular (LSM), and right submandibular (RSM) salivary glands had diameters; 16, 14, 11, and 12 mm, respectively. Technetium-99m solution (activity concentration; 300 kBq/mL) filled the salivary glands prior to implanting into a hollow head and neck phantom later filled with the technetium-99m solution (activity concentration; 1440 Bq/mL). A SPECT image was acquired on 128 × 128 matrix size over 30 min and reconstructed using filtered back projection algorithm (Butterworth filter with a cut-off frequency of 0.9 cycles per pixel and an order of 9). Reconstructed images were quantified using ImageJ software.</p> <p>Results: The image counts extracted from the LP, RP, RMS, and LMS salivary glands SPECT images were 672 019, 494 842, 398 091, and 262 908, respectively after the quantification of PVEs, compared to 486 320, 347 534, 272 940, and 175 307 before the quantification of PVEs. The respective quantitative errors were 27%, 29%, 31%, and 33%.</p> <p>Conclusion: Quantification of PVEs allows recovery of image counts spread outside the image pixels leading to improved quantification.</p>
<p>Article history: Received: Nov 13, 2018 Accepted: Mar 01, 2019</p>	
<p>Keywords: SPECT Salivary Glands Radiation Therapy</p>	

► Please cite this article as:

Nyathi M. Quantification of Partial Volume Effects in Salivary Glands SPECT Images after Radiation Therapy of Head and Neck Tumors. Iran J Med Phys 2020; 17: 27-34.10.22038/ijmp.2019.35431.1446.

Introduction

Radical radiation therapy is the main treatment modality used during the management of nonsurgical head and neck tumors [1, 2]. The ultimate goal of radiation therapy is to destroy the cancer cells while causing minimal destruction of the healthy tissues [2]. However, the administration of ionizing radiation in the head and neck region inevitably delivers exposure to the salivary glands and other healthy tissues.

The irradiation of the salivary glands leads to structural degradation and loss of function. An acute inflammatory reaction can be observed soon after irradiation. This is accompanied by a rapid loss of acinar cells leading to the development of xerostomia [1, 3]. The latter is characterized by dryness in the mouth. However, xerostomia is not life-threatening despite the long-term complications experienced by survivors. Notable complications include swallowing problems, loss of taste and appetite, speech problems, and poor oral hygiene [1, 4, 5].

Xerostomia may be graded either subjectively or objectively [1]. Subjective grading relies on the patient's description of the symptoms at the time of seeking medical assistance. However, the patient's assessment of xerostomia fails to give the clinician a definitive representation of the degree (extent) of xerostomia [6]. Therefore, an objective technique is required in order for clinicians to accurately grade xerostomia.

Traditionally, the salivary gland function was evaluated using salivary gland scintigraphy [1, 6-10]. Among the merits of the salivary gland scintigraphy technique is its reproducibility and none-invasive nature [1, 6]. Furthermore, salivary gland scintigraphy allows the simultaneous evaluation of both the parotid and the submandibular salivary glands [1, 6-11].

Salivary gland scintigraphy relies on the use of planar images of salivary glands. Qualitative functional information is deduced from time-activity

*Corresponding Author: Tel: 0027 780 203216; E-mail: Mpumelelo.Nyathi@smu.ac.za

curves generated from regions of interest drawn on each individual salivary gland [8, 9]. The technique was later improved with the introduction of semi-quantitative parameters [6, 10]. However, the technique still remains unstandardized.

A recent study carried out by Nyathi et al. [11], improved quantification by introducing a technique for quantifying partial volume effects (PVEs) on planar scintigraphy images.

The PVEs are attributed to the limited resolution of the gamma camera imaging system [12-14]. They are a phenomenon of structures with diameters two-three times lower than the resolution of the imaging system. They may manifest as spill-out or spill-in effects [14].

The spill-out effects lead to the spreading of the signal from inside the organ of interest to the background leading to the underestimation of the regional distribution of activity. On the contrary, spill-in effects are the results of activity moving from the background or adjacent organs into the organ of interest resulting in overestimation [13, 14]. In the presence of background activity, both effects occur simultaneously. Some background activity counts cancel out some activity counts originating from the targeted organ resulting in the reduction of the overestimated activity counts [12, 13]. In addition to dependence on the spatial resolution, PVEs are dependent on object size, shape, and activity concentration inside the organ relative to its surrounding [13].

Irradiated salivary glands in radiation injury may shrink in size due to the loss of acinar cells which die as a result of radiation injury. The salivary glands become prone to PVEs during imaging due to their reduced size. The activity-time curves generated from each individual salivary gland fail to give a true reflection of the activity counts. Therefore, the functional information derived from the time-activity curves is not accurate.

In an attempt to improve quantification, Nyathi et al. [11], quantified the PVEs in salivary gland scintigraphy. However, the superposition of structures presents challenges, which are highly likely to falsify the quantitative factors. In order to overcome the above-mentioned challenges, the present study proposed the use of single-photon emission computed tomography (SPECT) technique with a component of PVEs quantification. The advantage of SPECT technique is that the imaged salivary glands can be viewed in the form of slices in the coronal, sagittal or transverse planes. This allows the clinician to select slices on the particular plane and quantify PVEs. The additional advantage of the SPECT technique is its ability to separate overlapping structures [15].

This study introduced a PVEs quantification technique that aimed at recovering image counts spread outside the image pixels of SPECT images of each individual parotid and submandibular salivary

glands post radiation therapy of head and neck tumors.

Materials and Methods

Hollow spheres (Figure 1) were improvised to mimic salivary glands before and after radiation therapy. The diameters of the salivary glands were 16, 14, 12, and 11 mm for the left parotid salivary gland (LP), right parotid salivary gland (RP), right submandibular gland (RSM), and left submandibular salivary gland (LSM), respectively.



Figure 1. Hollow spheres mimicking two major pairs of salivary glands, namely parotid and submandibular salivary glands

The spheres LP and RMS in Figure 1 mimic intact salivary glands, while the spheres RP and LMS mimic the salivary glands with reduced size due radiation injury. The reduction in size of injured salivary glands is attributed to loss of acinar cells that got depleted as a result of death after radiation injury. Four salivary glands were filled with the technetium-99m solution (activity concentration of 300 kBq/mL) and then implanted inside a hollow head and neck phantom (Figure 2) using insoluble wax. Polystyrene rods were used to support the submandibular salivary glands.



Figure 2. Side view of head and neck phantom

A solution of technetium-99m (activity concentration of 1440 Bq/mL) was poured into the phantom through an opening on its base providing background activity for the salivary glands, and then the opening was sealed. The background activity was intended to match a clinical scenario in which there is always background activity in the blood pool during biodistribution of technetium-99m in the body post intravenous injection. With the head and neck phantom

placed in the supine position on the imaging table (Figure 3), SPECT projections of the phantom were acquired on a 128×128 matrix size over duration of 30 min using a Siemens E-Cam dual head gamma camera (Figure 3).



Figure 3. Head and neck phantom placed in supine position on imaging table during imaging

The gamma camera was programmed to a noncircular orbit. This motion facilitated the detector being as close as possible to the head and neck phantom during imaging. The acquired projections were

reconstructed using a filtered backprojection algorithm (Butterworth filter with a cut-off frequency of 0.9 cycles per pixel and an order of 9). These parameters were observed to be optimal for noise reduction and image resolution recovery for images of structures with dimensions that are 2-3 times lower than the resolution of the gamma camera [15]. The two-dimensional (2D) transaxial image slices of both the parotid and submandibular salivary glands were quantified using ImageJ software following the application of the method proposed by Nyathi et al. [16]. Figure 4 depicts the small economic window of ImageJ software with a circular tool used in quantification and other tools available on ImageJ software.

With the use of the circular tool from ImageJ software, a region of interest (ROI) 1 was drawn on the image boundary of each gland with a radius equal to that of the gland measured using ImageJ software tool line command [16]. The ROI 1 extracted image counts before PVEs quantification. The ROI 2 was also added to each individual salivary gland image slice (Figures 5 and 6). This was drawn in a way that was extended from the boundary of ROI 1 by the FWHM (7 pixels which equated to 20.88 mm) of the gamma camera measured at a distance of 5 cm.

The ROI 2 included recovered image counts that were spread outside the image pixels due to PVEs. The difference between image counts in ROI 2 and ROI 1 gave the smeared image counts that were responsible for the underestimation of the regional distribution of activity in all the spheres.

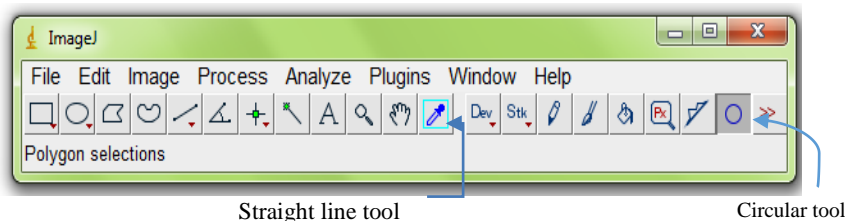


Figure 4. Demonstration of used tools for quantification of medical images by ImageJ window URL: <https://imagej.nih.gov/ij/download.html>

Results

Six 2D transaxial image slices of the submandibular salivary glands had quantifiable image counts, compared to nine 2D transaxial parotid salivary gland image slices. Figures 5 and 6 show ROI 1 and ROI 2 used to quantify the 2D transaxial slices of both the submandibular and parotid salivary glands, respectively.

The extracted image counts before and after the quantification of PVEs are presented in tables 1 and 2 for each individual submandibular salivary gland and each individual parotid salivary gland, respectively. The use of ROI 2 facilitated the recovery of image counts blurred through the walls of the salivary glands resulting in the underestimation of the regional distribution of the activity counts inside the glands.

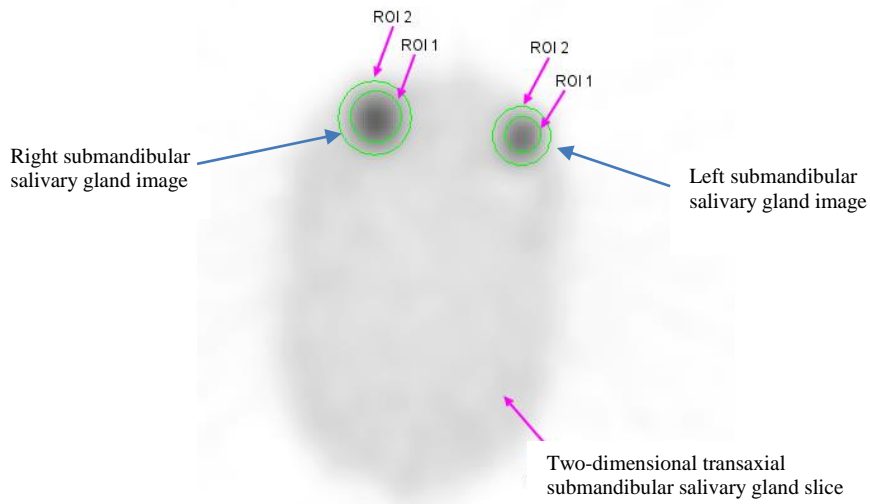


Figure 5. Use of region of interest 1 and region of interest (ROI) 2 to extract image counts on a two-dimensional transaxial submandibular salivary gland slice; quantification of partial volume effects by ROI 2 and recovery of image counts smeared outside the image pixels

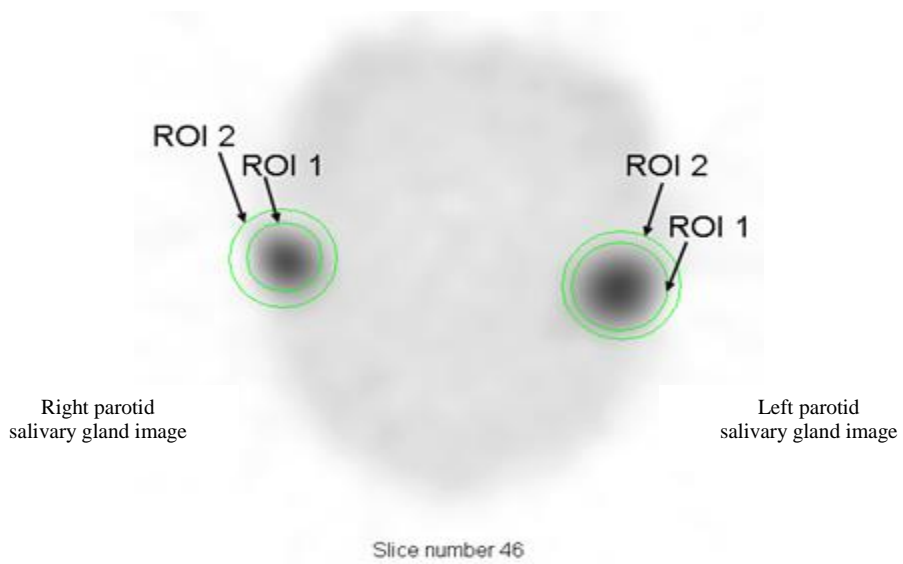


Figure 6. Use of region of interest 1 and region of interest (ROI) 2 to extract image counts on a two-dimensional transaxial parotid salivary gland slice; quantification of partial volume effects by ROI 2 and recovery of image counts smeared outside the image pixels

Table 1. Extraction of image counts from two-dimensional transaxial image slices of left and right submandibular glands before and after partial volume effects (PVEs) quantification

Submandibular Glands																		
Actual slice # as recorded in two-dimensional slice	Image Counts extracted from left salivary gland (LSM)									Image Counts extracted from right salivary gland (RSM)								
	Region of interest 1 (ROI 1) image counts [Measurement of image counts before PVEs quantification]			Region of interest 2 (ROI 2) image counts [Measurement of image counts after PVEs quantification]			Recovered image counts [Underestimated image counts spreading outside salivary gland] ROI 2 – ROI 1 image counts			Region of interest 1 (ROI 1) image counts [Measurement of image counts before PVEs quantification]			Region of interest 2 (ROI 2) image counts [Measurement of image counts after PVEs quantification] ROI 2 – ROI 1 image counts			Recovered image counts [Underestimated image counts spreading outside salivary gland] ROI 2 – ROI 1 image counts		
	Measurement			Measurement			Measurement			Measurement			Measurement			Measurement		
	One	Two	Three	One	Two	Three	One	Two	Three	One	Two	Three	One	Two	Three	One	Two	Three
35	0	0	0	0	0	0	0	0	0	46120	46120	46120	72024	72024	72024	25904	25904	25904
36	22331	22331	22335	36403	36403	36400	14072	14072	14065	73795	73795	73769	93749	93749	93749	19954	19954	19980
37	47948	47954	47975	65334	65340	65335	17386	17386	17360	45873	45873	45873	68354	68355	68354	22481	22482	22481
38	35633	35632	35426	53070	53071	52070	17437	17439	16644	53333	53338	53333	78182	78180	78182	24849	24842	24849
39	39295	39296	39295	62176	62175	62176	22881	22879	22881	53826	53826	53826	85782	85782	85782	31956	31956	31956
40	30157	30156	30157	46257	46256	46257	16100	16100	16100	0	0	0	0	0	0	0	0	0
Total slice count	175364	175369	175188	263240	263245	262238	87876	87876	87050	272947	272952	272921	398091	398090	398091	125144	125138	125170
Mean Slice Count	175307			262908			87601			272940			3980901			125151		
% underestimation				33%									31%					

Table 2. Extraction of image counts from two-dimensional transaxial image slices of the left and right parotid glands before and after partial volume effects (PVEs) quantification

Actual slice # as recorded in two-dimensional slice	Parotid Salivary Glands																	
	Image Counts extracted from Right Parotid Salivary Gland (RP)									Image Counts extracted from Left Parotid Salivary Gland (LG)								
	Region of interest 1 (ROI 1) image counts [Measurement of image counts before PVEs quantification]			Region of interest 2 (ROI 2) image counts [Measurement of mage counts after PVEs quantification]			Recovered Counts [Underestimated image counts spreading outside salivary gland] ROI 2 – ROI 1 image counts			Region interest 1 Counts [Measurement of image counts before PVEs quantification]			Region interest 2 (ROI 2) image counts [Measurement of image counts after PVEs quantification]			Recovered Counts [Underestimated image counts spreading outside salivary gland] ROI 2 – ROI 1 image counts		
	Measurement			Measurement			Measurement			Measurement			Measurement			Measurement		
	One	Two	Three	One	Two	Three	One	Two	Three	One	Two	Three	One	Two	Three	One	Two	Three
44	0	0	0	0	0	0	0	0	0	35379	35379	35380	45722	45722	45722	10343	10343	10342
45	42736	42734	42735	67785	67784	67785	25049	25050	25050	83396	83396	83397	100759	100759	100759	17363	17363	17362
46	55085	55085	55085	68058	68058	68057	12973	12973	12972	52825	52826	52827	84882	84882	84882	32057	32056	32055
47	40999	40999	41000	59611	59610	59611	18612	18611	18611	51492	59427	51493	69147	69147	69147	17655	9720	17654
48	58024	58025	58023	88656	88656	88655	30632	30631	30632	82428	81633	82428	122053	122053	122053	39625	40420	39625
49	63569	53571	53570	82102	82103	82102	18533	28532	28532	60635	48611	60635	96646	96646	96646	36011	48035	36011
50	45427	45427	45428	47667	47667	47668	2240	2240	2240	58612	58611	58612	75795	75795	75795	17183	17184	17183
51	48360	48360	48361	80964	80964	80964	32604	32604	32603	31498	31497	31498	38390	38390	38390	6892	6893	6892
52	0	0	0	0	0	0	0	0	0	31682	31681	31682	38625	38625	38625	6943	6944	6943
Total slice count	354200	344201	344202	494843	494842	494842	140643	150641	150640	487947	483061	487952	672019	672019	672019	184072	188958	184067
Mean slice count	347534			494842			147308			486320			672019			185699		
% Underestimation							29%									27%		

According to Table 1, it can be observed that the quantification error was higher for LSM salivary gland (33%), compared to that for RSM salivary gland (31%). The PVEs are known to affect more imaged objects with diameters that are 2-3 times lower than the resolution of the imaging system [13, 14]. The LSM salivary gland was more affected by PVEs, compared to the RSM salivary gland due to the fact that it is smaller. Similarly, based on Table 2, the quantification error was higher for the RP salivary gland (29%), compared to that for the LP salivary gland (27%) because the RP salivary gland was smaller than the LP salivary gland.

$$\text{Underestimation percentage} = \frac{\text{Recovered Image Counts (ROI 2-ROI 1 image counts)}}{\text{Image Counts measured after PVEs quantification (ROI 2 image counts)}} \times 100$$

Discussion

The novelty of this proposed PVEs quantification technique is its ability to recover the image counts spread outside the image pixels of the salivary glands images. Loss of the activity counts from the salivary glands contributed to the underestimation of image counts extracted from the SPECT images of the salivary glands as shown in Tables 1 and 2. According to Table 1, it can also be observed that without effecting PVEs quantification, image counts were underestimated. Moreover, the quantification error of image counts extracted from the LP salivary gland was 27%, while it was 29% for the RP salivary gland.

According the above-mentioned results in tables 1 and 2, it can be established that as the size of the salivary glands decreased, the quantification errors increased. This trend was also observed in the case of the right and left submandibular glands reported as 31%, and 33%, respectively. These findings are in agreement with the results of studies demonstrating that accurate quantification of activity in organs or objects with dimensions two-three times lower than the resolution of the imaging system is hindered by PVEs. The PVEs cause activity counts to blur through the wall of the organ resulting in the underestimation of counts from the acquired images [11-14].

This newly proposed PVEs quantification technique, salivary gland SPECT incorporating PVEs, is consequently a more robust technique capable of recovering the image counts associated with the displaced activity using ROI 2. The number of image counts from each individual salivary gland may be equated with the degree of its damage.

Previously, many PVEs quantification techniques have been developed commonly referred to as partial volume correction methods [13, 16, 17]. However, these techniques are not used in routine clinical practice owing to lack of standardization and uncertainty among clinicians regarding the adoption of the best technique. This is despite the increasing evidence demonstrating that PVE correction or PVEs quantification is significant in order to guarantee absolute quantification.

In a study carried out by Erlandsson et al. [13], it was observed that most PVEs correction methods relied on accurately registered anatomical data (preferably magnetic resonance imaging). However, such data are not always accessible, that results in hindering applications in clinical use. The present study introduced a PVEs quantification technique that is cost-effective and relies on license-free software (ImageJ). The software can be downloaded free of charge from the web [18]. Furthermore, the advantage of ImageJ software is that it is supported by a large number of community users. Consistent updates of the software are periodically performed.

All PVE techniques aim at reversing the effect of the limited resolution of the imaging system. They tend to restore the true activity distribution of small structures with diameters 2-3 times lower than the spatial resolution of the imaging system as measured by the FWHM of the point spread function of the point source. In this study, the successful application of ImageJ software was managed to restore true image counts of the SPECT images of individual salivary glands using two regions of interest.

As shown in figures 4 and 5, ROI 2 extracted true image counts that make accurate quantification a reality. It is proposed that future patients should undergo salivary gland SPECT imaging before the treatment of head and neck tumors, and then the function of their glands be quantified. The obtained quantitative values will constitute a baseline. After the treatment, the patients should also undergo a second round of salivary gland SPECT imaging.

A comparison of the image counts for each individual gland before and after the treatment will provide the clinician with a precise diagnosis about the degree of the individual salivary gland injury. The degree of damage can then be associated with the number of extracted image counts. The lower the image counts were extracted from the 2D slice, the more damaged the salivary gland will be. Different dimensions of the pair of the salivary glands were used to illustrate this fact. The RP and LSM spheres mimicked salivary glands severely injured during radiation, while the LP and the RSM spheres mimicked intact salivary glands that were not damaged or minimally damaged by ionizing radiation during the therapy. The advantage of salivary gland SPECT with PVEs quantification is that it is a digital technique with the ability to detect minor changes in parenchyma.

In addition to its flexibility to evaluate the function of salivary glands after radiation therapy, this proposed PVEs quantification technique can be applied in other clinical settings. In a study conducted by Bardies and Buvat [19], it was established that PVE quantification can be useful for dose monitoring in tumors and organs at risks among the patients treated with targeted radiotherapy. Tumors are most likely to shrink in treatment and become prone to PVEs. Therefore, the --

ability to quantify PVEs is essential during the assessment of tumor response to therapy.

Conclusion

ImageJ software offers an opportunity to recover image counts spread outside the image pixels of salivary glands due to the limited resolution of the imaging system. The ImageJ software can be installed on a personal laptop or workstation and is license-free. As a result it is easily accessible to all clinicians in their work stations. This software makes it possible to achieve improved quantification of SPECT images. Ability to quantify PVEs will indeed restore true activity distribution in small structures with diameters 2-3 times lower than the spatial resolution of the imaging system as measured by the FWHM of the point spread function of the point source.

Acknowledgment

The author acknowledges with great appreciation Nkosi Maphumulo then Medical Physics intern at Dr George Mukhari Academic Hospital (DGMAH) for his assistance he rendered during the imaging session and DGMAH for allowing the author to use their equipment.

References

- Gupta T, Hotwani C, Kannan S, Master Z, Rangaranjan V, Murthy V, et al. Prospective longitudinal assessment of the parotid gland function using dynamic quantitative pertechnetate scintigraphy and estimation of dose-relationship of radiotherapy in head and neck. *Radiation Oncology*. 2015; 10:67.
- Cheng SC, WU VWC, Kwong DLW, Ying MTC. Assessment of post-radiotherapy salivary gland. *Brit J Radiol*. 2011; 84:393-402.
- Ahmed NS, Mansour SM, El-Wakd MM, Al-Azizi HM, Abu-Taleb NS. The value of magnetic resonance sialography and magnetic resonance imaging versus conventional sialography of the parotid gland in the diagnosis and staging of Sjogren's syndrome. *The Egyptian Rheumatologist*. 2011; 33:147-54.
- Clarke HD, Moiseenko VV, Rackley TP, Thomas SD, W JS, Reinsberg SA. Development of a method for functional identification of parotid using dynamic contrast-enhanced magnetic resonance. *Imageing and concurrent stimulation*. *Acta Oncologia*. 2015;54(9):1686-90.
- Jimenez - Heffernan A, Gomez - Millan J, De Mora ES, Moreno JD, Gil MM, Salgo C, et al. Quantitative salivary gland scintigraphy in the head and neck cancer patients following radiotherapy. *Rev Esp Med Nucl*. 2010; 29(4):165-71.
- Knoll P, Krtla G, Bastati B, Koriska K, Mirzaei S. Improved quantification of salivary gland scintigraphy by means of factor analysis. *Iran J Nucl Med*. 2012; 20(1):5-10.
- Vinagre F, Santos Mj, Prata A, Canas da Silva J, Santos AI. Assessment of salivary glands function in Sjogren's syndrome: salivary gland scintigraphy. *Autoimmunity Reviews*. 2009; 8:672-6.
- Dugonjić S, Stefanović D, Đurović B, Spasić V. Evaluation of diagnostic parameters from parotid and submandibular dynamic salivary glands scintigraphy and unstimulated sialometry in Sjögren's syndrome. *Hell J Nucl Med*. 2014; 17(2): 116-22.
- Loutfi I, MD, Nair MK, Ali K. Ebrahim AK. Salivary Gland Scintigraphy: The Use of Semiquantitative Analysis for Uptake and Clearance. *J Nucl Med Technol*. 2003; 31:81-5.
- Angusti T, Pilati E, Parente A, Carignola R, Manfredi M, Cauda S, et al. Semi-quantitative analysis of salivary gland scintigraphy in Sjogren's syndrome diagnosis: a first-line tool. *Clinical Investigations*. 2017; 21(7):2389-95.
- Nyathi M, Sithole ME. Salivary glands scintigraphy with partial volume effects quantification: A phantom feasibility study. *AMJ*. 2017; 10(9):752-8.
- Lehnert W, Gregoire MC, Reilhac A, Meikle SR. Characterisation of partial volume effect and region-based correction in small animal positron emission tomography (PET) of the rat brain. *Neuroimage*. 2012; 61:2144-57.
- Erlandsson K, Buvat I, Hendrik Pretorius PH, Benjamin A, Thomas BA, Hutton BF. A review of partial volume correction techniques for emission tomography and their applications in neurology, cardiology and oncology. *Phys Med Biol*. 2012; 57: 119-59.
- Ritt P, Vija H, Hornegger J, Kuwert T. Absolute quantification in SPECT. *Eur J Nucl Med Mol Imaging*. 2011; 38: 68-77.
- Groch MW, Erwin WD. SPECT in the year 2000: Basic principles. *J Nucl Med Technol*. 2000; 28(4):233-44.
- M. Nyathi. Quantitative evaluation of the parotid and submandibular salivary glands function post radiation therapy of head and neck tumors. PhD thesis. Ga-Rankuwa. South Africa. 2015.
- Nyathi M, Sithole ME, Ramafi OE. Quantification of Partial volume effects in planar imaging. *Iran J Nucl Med*. 2016; 24(2):116-20.
- ImageJ bundled with 64-bit Java 1.8.0_112. Available from: <https://imagej.nih.gov/ij/download.html>.
- Bardies M and Buvat I. Dosimetry in nuclear medicine therapy: what are the specifics in image quantification for dosimetry? *Quarterly Journal of Nuclear Medicine and Molecular Imaging*. 2011;55(1):5.